IETA International Information and Engineering Technology Association

International Journal of Heat and Technology

Vol. 43, No. 5, October, 2025, pp. 1963-1972

Journal homepage: http://iieta.org/journals/ijht

Thermodynamic Behavior and Difference Analysis of Nitrogen and Phosphorus Adsorption by Zeolite Modified with Different Reagents



Ziyu Liu¹, Tiejian Zhang¹, Zhihua Bian², Junliang Liu¹

- ¹ Urban Construction Institute, Hebei Agricultural University, Baoding 071001, China
- ² Hebei Xiong'an Yushuo Technology Co., Ltd., Xionganxingu 070001, China

Corresponding Author Email: cjztj@hebau.edu.cn

Copyright: ©2025 The authors. This article is published by IIETA and is licensed under the CC BY 4.0 license (http://creativecommons.org/licenses/by/4.0/).

https://doi.org/10.18280/ijht.430535

Received: 2 September 2025 Revised: 18 October 2025 Accepted: 25 October 2025

Available online: 31 October 2025

Keywords:

clinoptilolite zeolite, modifiers, nitrogen and phosphorus adsorption, adsorption thermodynamics, adsorption mechanism, water pollution control

ABSTRACT

Eutrophication caused by nitrogen and phosphorus pollution has become a global environmental concern. Traditional removal methods, such as biological treatment and chemical precipitation, often face challenges like high costs and secondary pollution. Clinoptilolite, a natural low-cost zeolite, has attracted attention due to its ion exchange capacity and porous structure, but its low phosphorus adsorption and limited nitrogen selectivity restrict wider application. This study investigates how inorganic, organic, and composite modifiers regulate the structure and surface properties of clinoptilolite and explores their effects on the thermodynamics of ammonium (NH₄+-N) and phosphate (PO₄³⁻-P) adsorption. Modified zeolites—iron-modified (Fe-Z), cetyltrimethylammonium bromide-modified (CTAB-Z), and iron-CTAB composite-modified (Fe-CTAB-Z)—were prepared via impregnation or ion exchange. Characterization was conducted using XRD. SEM, BET, FTIR, XPS, and zeta potential analysis. Adsorption isotherms were measured at 298 K, 308 K, and 318 K, and thermodynamic parameters (ΔG^0 , ΔH^0 , ΔS^0) were calculated using Langmuir, Freundlich, and Dubinin-Radushkevich models and the Van't Hoff equation. Results showed significant adsorption selectivity: Fe-Z achieved a maximum NH₄+-N capacity of 20.5 mg/g (138% higher than raw zeolite), while Fe-CTAB-Z reached 15.8 mg/g for PO₄³-P (a 778% increase), highlighting the synergistic effect of composite modification on phosphorus adsorption. All modified zeolites exhibited spontaneous, endothermic adsorption ($\Delta G^0 < 0$, $\Delta H^0 > 0$). Notably, Fe-CTAB-Z had a ΔH^0 of 28.6 kJ/mol for PO₄³⁻-P, indicating enhanced adsorption strength. D-R model analysis revealed chemical adsorption for Fe-Z and Fe-CTAB-Z (E = 10.2-12.5 kJ/mol), while CTAB-Z showed physical adsorption (E < 8 kJ/mol). Structural analysis confirmed that modifiers influenced adsorption spontaneity and stability by altering pore structure, introducing functional groups, and modifying surface charge. This study provides thermodynamic insights for designing nitrogen/phosphorus-selective adsorbents and advancing zeolite applications in water pollution control.

1. INTRODUCTION

Excessive nitrogen and phosphorus emissions leading to eutrophication of water bodies have become a global water environmental crisis. According to the latest survey data, more than 60% of freshwater lakes and 45% of reservoirs worldwide are under varying degrees of eutrophication stress. The frequent occurrence of cyanobacterial blooms not only causes depletion of dissolved oxygen in water and massive mortality of aquatic organisms, but also releases secondary pollutants such as microcystin toxins, which directly threaten drinking water safety and ecosystem services [1, 2]. In traditional nitrogen and phosphorus removal technologies, biological treatment methods are poorly adapted to low-temperature and low-concentration water, while chemical precipitation methods generate large amounts of sludge, leading to secondary pollution. Adsorption methods, on the other hand, have become a core research direction in the field of deep water purification due to their advantages of simple operation, controllable cost, and material recyclability [3, 4]. Clinoptilolite, as the most abundant natural zeolite in the Earth's crust, has shown great potential for pollutant adsorption due to its unique three-dimensional framework structure, excellent ion-exchange properties, and low acquisition cost. However, the raw material has significant performance defects: the inherent negative charge on its surface leads to strong electrostatic repulsion against phosphate ions (PO₄³⁻-P), and it lacks specific adsorption sites for phosphorus, with a typical maximum adsorption capacity for PO₄³⁻-P usually less than 2 mg/g [5, 6]. Meanwhile, cations such as Ca²⁺ and Mg²⁺ coexisting in the pore channels compete for exchange sites with ammonium nitrogen (NH₄+-N), resulting in insufficient selectivity for nitrogen adsorption. Therefore, modifying the zeolite's structure and surface properties has become the key to overcoming its performance limitations [7]. However, most existing studies focus on the effect of single modifiers on the adsorption of nitrogen or phosphorus components separately [8-10], lacking systematic comparisons of the thermodynamic behavior of nitrogen and phosphorus co-adsorption using inorganic, organic, and composite modifiers. Moreover, how modification alters the zeolite's crystal structure, pore characteristics, surface charge, and other properties to quantitatively regulate thermodynamic parameters such as enthalpy change (ΔH^0) and entropy change (ΔS^0) remains unclear, greatly limiting the targeted design and engineering application of efficient modified materials.

Zeolite modification technologies have formed three major mature systems: inorganic, organic, and composite modifications. Inorganic modification improves performance by etching pores or introducing active sites. For example, acid modifications such as hydrochloric acid can dissolve pore impurities to increase surface area, enhancing NH₄+-N adsorption by 30%-50%. Metal ions such as Fe³⁺ and Al³⁺ can be impregnated to introduce coordination sites, with Fe3+modified zeolite achieving adsorption of PO₄³⁻-P up to 6-8 times that of the raw material [11, 12]. Organic modification, such as using quaternary ammonium salts and chitosan, regulates surface charge. CTAB, as a typical quaternary ammonium salt, can be ion-exchanged onto the zeolite surface, reversing the Zeta potential from negative to positive, thus enhancing electrostatic adsorption of PO₄³⁻-P, although pore blockage may reduce NH₄⁺-N adsorption performance [13]. Composite modifications, such as Fe³⁺-CTAB, enhance nitrogen and phosphorus adsorption performance through synergistic effects of pore formation and charge modification, outperforming single-modifier systems. However, most related studies focus on performance characterization, with insufficient analysis of the relationship between modification mechanisms and thermodynamic behavior [14]. In terms of adsorption thermodynamics, the Langmuir, Freundlich, and Dubinin-Radushkevich models are used to fit monolayer adsorption, heterogeneous adsorption, and distinguish physical/chemical adsorption [15, 16]. Parameters such as Gibbs free energy change (ΔG^0), enthalpy change (ΔH^0), and entropy change (ΔS^0) reveal the spontaneity, thermal effects, and changes in system disorder during adsorption [17, 18]. However, current research shows significant gaps: most studies only calculate parameters based on single-temperature data, ignoring the potential adsorption mechanism changes triggered by increasing temperature, which leads to deviations in parameter interpretation. Additionally, there is a lack of quantitative explanations for the thermodynamic differentiation caused by modifier differences, such as the ΔH^0 difference of 10-15 kJ/mol between Fe3+ and Al3+-modified zeolites, and its relationship with surface functional group types and coordination bond strength remains unclear [19, 20].

To address the above research gaps, this paper aims to clarify the relationship mechanism between "modification strategy - material structure - adsorption thermodynamics" and break through the bottleneck of nitrogen and phosphorus adsorption selectivity in clinoptilolite. FeCl₃-modified Fe-Z, CTAB-modified CTAB-Z, and FeCl₃-CTAB composite-modified Fe-CTAB-Z zeolites were prepared using impregnation or ion-exchange methods. Raw zeolite (Raw-Z) was used as a control, constructing a systematic comparison of "single modification - composite modification - raw material." The modification effects on material physicochemical properties were analyzed from the perspectives of crystal structure, morphology, pore channels, functional groups, and charge characteristics using XRD, SEM, BET, FTIR, XPS,

and Zeta potential testing. Adsorption experiments were conducted at three temperatures (298K, 308K, and 318K), and thermodynamic parameters were calculated by fitting with the Langmuir model and using the Van't Hoff equation, quantifying differences in adsorption capacity, affinity, and energy changes for NH₄⁺-N and PO₄³⁻-P in different modified systems. Based on the correlation analysis of "characterization parameters - adsorption performance - thermodynamic data," the intrinsic mechanisms of modifier regulation of nitrogen and phosphorus adsorption thermodynamics were revealed.

The main innovations of this study are: first, focusing on the selective differences in nitrogen and phosphorus adsorption, constructing four groups of control systems with inorganic, organic, composite modifications, and raw materials, systematically clarifying the relationship modification type and thermodynamic characteristics, filling the gap in the "selectivity mechanism" explanation in singlemodifier studies; second, combining post-adsorption XPS fine spectra and Zeta potential tests to establish a quantitative structure-activity relationship between "active site density surface charge intensity - thermodynamic parameters," breaking the limitations of purely performance-based descriptions; third, adopting the D-R model combined with multi-temperature experimental methods to accurately distinguish the contributions of physical and chemical adsorption, providing direct support for the mechanistic interpretation of parameters such as ΔH^0 .

The paper follows a logical structure of Methods, Results, Discussion, and Conclusions. Chapter 2 describes the preparation of modified zeolites, material characterization, adsorption experiments, and data processing to ensure reproducibility. Chapter 3 presents the characterization results, adsorption isotherms, and thermodynamic parameters, with an emphasis on the synergistic mechanism of Fe-induced pore formation and CTAB-driven surface charge regulation in nitrogen and phosphorus adsorption. Comparative analysis with existing literature is also included. Chapter 4 summarizes the main findings, clarifies application scenarios for Fe-Z in high-ammonium water and Fe-CTAB-Z in high-phosphorus water, and proposes future optimization directions. The study offers theoretical and technical support for the targeted design of modified zeolites and precise nitrogen/phosphorus control in water treatment.

2. MATERIALS AND METHODS

Figure 1 shows the technical route of the adsorption thermodynamic study of nitrogen and phosphorus by modified clinoptilolite. This figure clearly presents the entire process of this study: starting from the pre-treatment of natural clinoptilolite, conducting single-factor experiments and process optimization for inorganic FeCl₃, organic CTAB, and composite Fe-CTAB modifications, followed by material structure analysis using SEM, BET, etc. Afterward, multi-temperature nitrogen and phosphorus adsorption isotherm experiments and model fitting were performed to ultimately clarify the adsorption thermodynamic mechanisms of modified clinoptilolite for nitrogen and phosphorus.

2.1 Experimental materials

The natural clinoptilolite used in this study was collected from the zeolite mining area in Lingshou County, Hebei Province. To ensure the reproducibility and stability of the adsorption experiments, the raw material was standardized for pre-treatment. First, it was initially crushed using a jaw crusher, then screened to obtain particles of 200 mesh using a standard sieve. The particles were then repeatedly washed with distilled water until the filtrate pH stabilized and the conductivity was below 5 uS/cm, removing soluble impurities and fine dust attached to the surface. Afterward, the material was dried in a 105°C hot air oven for 4 hours, followed by drying in a 60°C vacuum oven for 24 hours to completely remove any residual moisture from the pore channels, and then sealed and stored for later use. The main elemental analysis of the pre-treated clinoptilolite was performed using an X-ray fluorescence spectrometer. The results showed that its main chemical composition was: SiO₂ 68.24%, Al₂O₃ 12.56%, CaO 3.82%, MgO 2.15%, Fe₂O₃ 1.98%, K₂O 2.74%, Na₂O 1.32%, with the remaining trace elements accounting for less than 5%. This composition conforms to the typical silico-aluminate framework characteristics of clinoptilolite. The modifiers and reagents used in the experiment, including Ferric chloride hexahydrate FeCl₃·6H₂O and Cetyltrimethylammonium bromide CTAB, were of analytical grade and purchased from Sinopharm Chemical Reagent Co., Ltd. Ammonium chloride NH₄Cl and Potassium dihydrogen phosphate KH₂PO₄ were of extra pure grade, while Hydrochloric acid HCl and Sodium hydroxide NaOH were of analytical grade, all purchased from Shanghai Aladdin Biochemical Technology Co., Ltd. All reagents were not further purified before use. The experimental water was ultrapure water prepared using a Milli-Q ultrapure water system with a constant resistivity of 18.2 M Ω ·cm to avoid interference from impurity ions during the adsorption process.

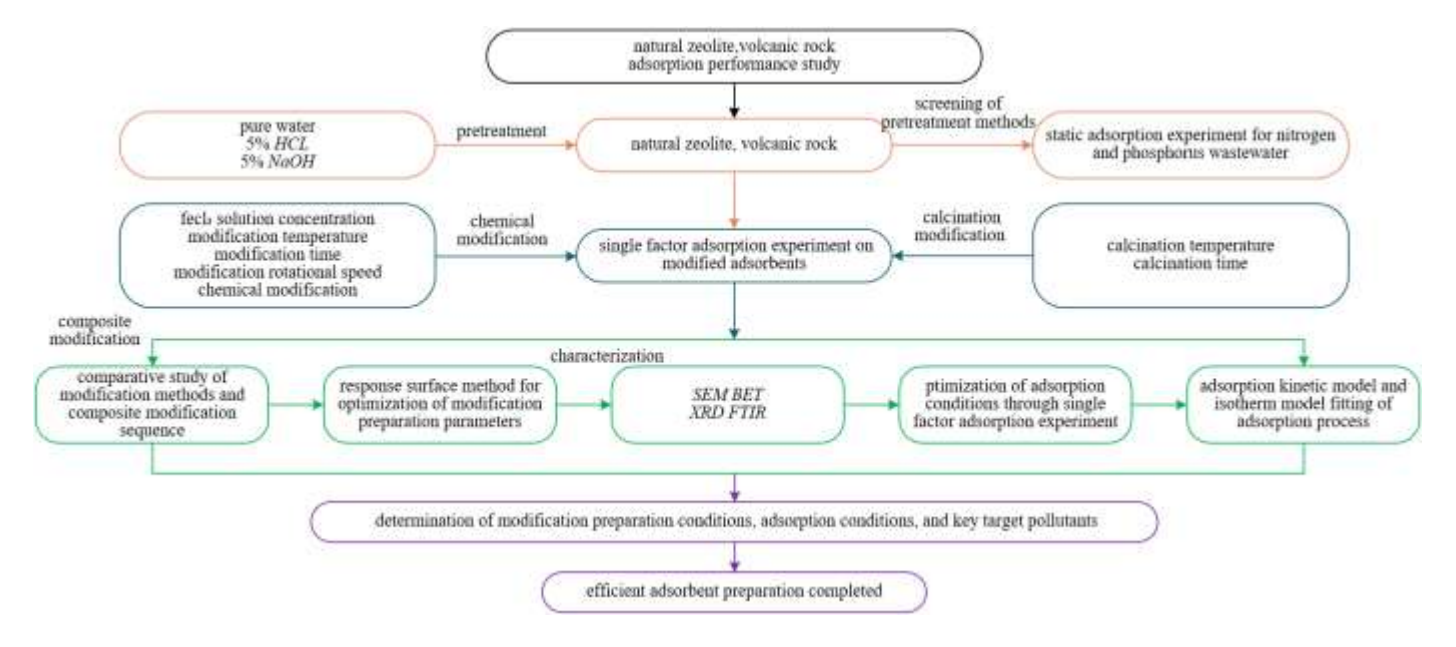


Figure 1. Technical route of adsorption thermodynamic study of nitrogen and phosphorus by modified clinoptilolite

2.2 Preparation of modified zeolites

In this study, three types of modified clinoptilolite were prepared using differentiated methods to achieve targeted control over material structure and surface properties. The inorganic modified zeolite Fe-Z was prepared by the impregnation-calcination method: 10.0 g of pretreated clinoptilolite was accurately weighed, and 50 mL of 0.3 mol/L FeCl₃ solution, optimized in a preliminary experiment, was added. The pH of the system was adjusted to 3.0 using 0.1 mol/L HCl or NaOH, and the mixture was then placed in a 30°C constant temperature water bath shaker at 150 rpm for 24 hours to ensure sufficient diffusion of Fe3+ onto the zeolite surface and into the pores. After the reaction, the mixture was filtered using a Büchner funnel and washed with distilled water until no Cl⁻ ions were detected in the filtrate. It was then dried at 105°C for 8 hours and calcined at 500°C for 2 hours in a muffle furnace to enhance the chemical bonding of Fe³⁺ with the zeolite framework. After cooling, the product was ground and passed through a 100-mesh sieve for later use.

The organic modified zeolite CTAB-Z was prepared by ion-exchange method to regulate the surface charge characteristics of the material: 10.0 g of pretreated clinoptilolite was weighed, and 50 mL of 0.1 mol/L CTAB solution, optimized for this purpose, was added. The mixture was placed in a 40°C

constant temperature water bath shaker at 120 rpm for 12 hours, allowing CTAB molecules to be ion-exchanged and loaded onto the zeolite surface and in the pores. After filtration, the zeolite was washed with distilled water until no residual surfactant was detected in the filtrate, then dried in a 60°C vacuum drying oven for 12 hours. This temperature was chosen to prevent thermal decomposition of CTAB, resulting in the positively charged CTAB-Z. The Zeta potential of CTAB-Z shifted from negative to positive compared to the raw zeolite, which significantly enhanced its electrostatic adsorption capacity for PO₄³--P.

The composite modified zeolite Fe-CTAB-Z was prepared using a two-step method to integrate the synergistic advantages of inorganic and organic modifications: Fe-Z was first prepared according to the inorganic modification process described above. Then, 5.0 g of Fe-Z was taken as the carrier, and 25 mL of 0.1 mol/L CTAB solution was added. The mixture was placed in a 35°C constant temperature water bath shaker at 150 rpm for 18 hours, allowing CTAB to be further loaded onto the Fe-Z surface via ion-exchange. The subsequent processing steps were identical to those for organic modification, i.e., filtration, washing to remove residual surfactants, and drying at 60°C in a vacuum for 12 hours. This process introduces Fe³⁺ coordination sites first, followed by surface modification with positively charged CTAB. This

maintains the chemical adsorption ability of Fe-Z for PO₄³-P while enhancing the adsorption force through CTAB's charge regulation. The porous structure of Fe-Z also alleviates the pore-blocking effect of CTAB, resulting in synergistic enhancement of nitrogen and phosphorus adsorption performance.

2.3 Material characterization methods

XRD analysis was performed using a Bruker D8Advance diffractometer with CuK α radiation, wavelength $\lambda=0.154$ nm, tube voltage 40 kV, and current 40 mA. The scanning range was set to $2\theta=5^{\circ}-80^{\circ}$, with a step size of 0.02° and a scanning speed of $5^{\circ}/min$. The diffraction patterns were obtained to analyze the impact of modification on the crystal structure of clinoptilolite. The intensity changes of the characteristic diffraction peaks of clinoptilolite at $2\theta=9.8^{\circ}, 11.3^{\circ},$ and 22.5° were particularly focused on. The crystallite size was calculated using the Scherrer equation, and the changes in interplanar spacing were examined to determine whether the modifier disrupted the integrity of the zeolite framework.

SEM observations were performed using a Zeiss Sigma 300 field emission scanning electron microscope at an accelerating voltage of 15 kV and working distance of 8 mm. The samples were coated with gold before observation in secondary electron mode. Images were taken at magnifications of 500×, 2000×, and 5000× to analyze surface roughness, pore distribution, and modifier loading states: the compactness of the raw zeolite surface, the attachment of Fe oxide particles on the Fe-Z surface, the thickness of the organic coating layer on the CTAB-Z surface, and the synergistic attachment of Fe oxide and CTAB in Fe-CTAB-Z. The morphological differences were linked to the impact of pore structure changes on adsorption mass transfer.

Surface area and pore size analysis were conducted using a Micromeritics ASAP2460 physical adsorption analyzer, with liquid nitrogen at 77K as the adsorbate and nitrogen gas as the adsorbent. Before testing, the samples were degassed at 300°C under vacuum for 6 hours to remove surface-adsorbed moisture and impurities. The Brunauer-Emmett-Teller (BET) model was used to calculate the specific surface area (S_{BET}), and the Barrett-Joyner-Halenda (BJH) model was used to analyze the total pore volume (V_{total}) and average pore diameter (D_{avg}). Adsorption-desorption isotherm types and hysteresis loop patterns were recorded to assess the impact of modification on zeolite pore structure, providing an explanation for differences in adsorption capacity at the pore structure level.

FTIR spectroscopy analysis was carried out using a ThermoFisher NicoletiS50 spectrometer, with samples prepared using the KBr pellet method. The scanning range was set to 400–4000 cm⁻¹ with a resolution of 4 cm⁻¹ and 32 scans. The background-subtracted spectra were analyzed to identify the evolution of surface functional groups. Key absorption peaks were identified, including the -OH stretching vibration at 3430 cm⁻¹, the Si-O-Al stretching vibration at 1030 cm⁻¹, the Fe-O characteristic peak at 580 cm⁻¹ in Fe-Z, and the C-H stretching at 2920 cm⁻¹ and C-N stretching at 1480 cm⁻¹ in CTAB-Z. The peak intensity and shifts were used to quantify the changes in functional groups introduced by the modifiers.

XPS analysis was performed using a ThermoFisher *K-Alpha* XPS system with $AlK\alpha$ as the excitation source, operating at a power of 150 *W*. The vacuum pressure in the analysis chamber was below 1×10^{-9} Pa. Monochromatic X-

rays were used to acquire full spectrum and high-resolution narrow spectrum scans, with C1s as the internal standard for charge calibration. The full spectrum analysis was used to confirm the successful loading of modification elements such as Fe and N, and the presence of P elements after adsorption. The narrow spectrum focused on Fe2p, N1s, and P2p, and peak fitting of the characteristic peaks was performed to calculate the relative content of different oxidation states of elements. This allowed for the establishment of a link between surface chemical states and adsorption forces.

Zeta potential analysis was performed using a Malvern Zetasizer NanoZS potential analyzer at a concentration of 0.01 g/mL in ultrapure water. The sample was sonicated for 10 minutes before measuring the Zeta potential at each pH level, which was adjusted using 0.1 mol/L HCl or NaOH. Each pH gradient was equilibrated for 5 minutes before measurement, and the Zeta potential was measured in triplicate for each sample. The Zeta potential-pH curves were used to analyze the effects of modification on the zeolite surface charge, including changes in the isoelectric point and the positive or negative nature of the potential at different pH values. This analysis directly correlated surface charge with the electrostatic adsorption capacity for PO₄³--P, providing a theoretical basis for adsorption pH adaptability.

2.4 Data calculation

The equilibrium adsorption capacity is the fundamental parameter for evaluating the adsorption performance of modified zeolite. It is calculated by measuring the change in nitrogen and phosphorus concentrations in the solution before and after adsorption, using the following formula:

$$q_e = \frac{\left(C_0 - C_e\right)V}{m} \tag{1}$$

where, C_0 is the initial concentration, C_e is the equilibrium concentration, V is the volume of the solution, and m is the mass of the adsorbent. This parameter directly reflects the actual nitrogen and phosphorus capture capacity of the modified zeolite per unit mass, and serves as a quantifiable index for comparing the effectiveness of different modification schemes.

The calculation of adsorption thermodynamic parameters is the core analytical method of this study. These parameters can reveal the spontaneity, energy change, and entropy change characteristics of the adsorption process:

The Gibbs free energy change ΔG^0 is calculated by the following equation:

$$\Delta G^0 = -RT \ln K_L \tag{2}$$

where, K_L is the Langmuir adsorption constant, R is the gas constant, and T is the absolute temperature. A negative value of ΔG^0 indicates that the adsorption process is spontaneous, and the larger the absolute value, the stronger the driving force. In this study, ΔG^0 is used to compare the spontaneity of nitrogen and phosphorus adsorption on different modified zeolites, with a particular focus on how temperature affects ΔG^0 , revealing how the introduction of modifiers alters the thermodynamic driving force of adsorption.

The enthalpy change ΔH^0 and entropy change ΔS^0 are calculated using the Van't Hoff equation:

$$\ln K_L = -\frac{\Delta H^0}{RT} + \frac{\Delta S^0}{R} \tag{3}$$

By plotting lnK_L against 1/T, the slope and intercept of the fitted line can be obtained. The sign of ΔH^0 distinguishes between endothermic and exothermic processes, while ΔS^0 reflects the change in the degree of disorder at the interface. These parameters are used to analyze how modification changes the thermal effects of adsorption and the entropy change at the interface, providing thermodynamic support for understanding the adsorption mechanism.

The calculation of these thermodynamic parameters not only quantifies the differences in nitrogen and phosphorus adsorption capacities of modified zeolites but also reveals the essential characteristics of the adsorption process, providing theoretical support for subsequent adsorption mechanism analysis.

2.5 Model fitting

To gain a deeper understanding of the adsorption mechanisms of modified zeolites for nitrogen and phosphorus, this study uses three classic adsorption models to fit the adsorption isotherms at different temperatures. Figure 2 presents a schematic diagram of the adsorption models for modified clinoptilolite on nitrogen and phosphorus. This diagram visually illustrates the adsorption mechanisms of Langmuir monolayer adsorption, Freundlich heterogeneous surface adsorption, and D-R physical/chemical adsorption, along with the adsorption behavior of nitrogen and phosphorus ions on the surface and in the pores of modified zeolite based on the micropore structure characteristics of clinoptilolite.

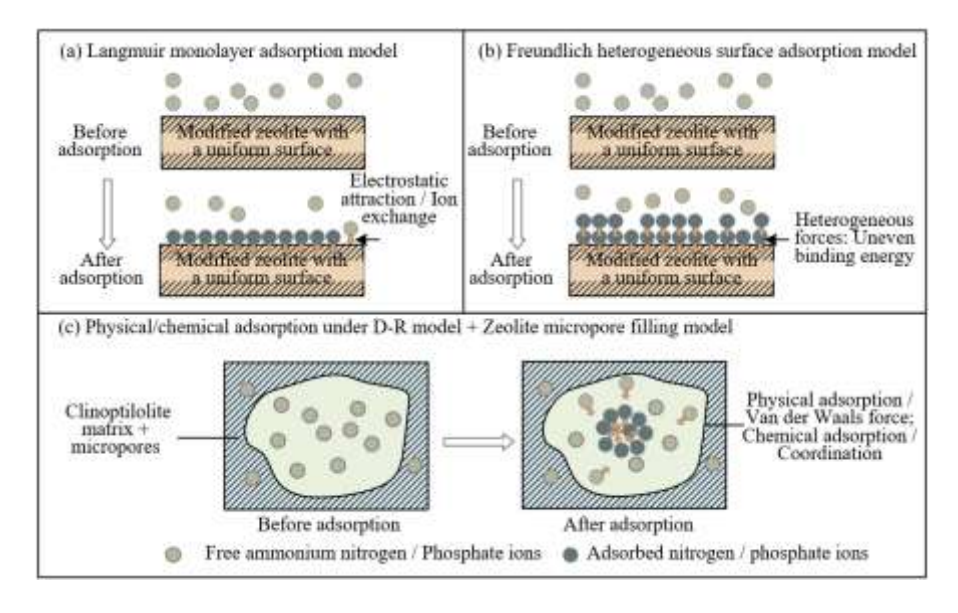


Figure 2. Schematic diagram of adsorption models for modified clinoptilolite on nitrogen and phosphorus

The Langmuir model assumes that the adsorbent surface is homogeneous and forms a monolayer adsorption, suitable for evaluating the maximum adsorption capacity and adsorption affinity of modified zeolite. The maximum adsorption capacity q_m obtained from the fitting can directly compare the differences in adsorption capacity between different modification schemes, and K_L reflects the interaction intensity between the adsorbent and the adsorbate. The specific model expression is:

$$\frac{C_e}{q_e} = \frac{1}{q_m K_L} + \frac{C_e}{q_m} \tag{4}$$

The Freundlich model is suitable for multilayer adsorption on heterogeneous surfaces. Its parameters K_F and 1/n reflect the adsorption capacity and adsorption strength, respectively. When this model fits better than the Langmuir model, it suggests that the modification may have resulted in the formation of energy-uneven adsorption sites on the zeolite surface, which is crucial for understanding the complex nitrogen and phosphorus adsorption process. The specific model expression is:

$$\ln q_e = \ln K_F + \frac{1}{n} \ln C_e \tag{5}$$

The D-R model distinguishes physical adsorption from chemical adsorption by calculating the average adsorption energy $E=1/(2\beta)^{1/2}$, which is a key tool for revealing the modification mechanism. By analyzing the variation of E, it is possible to clarify how different modification schemes alter the nature of the adsorption force, providing direct evidence for explaining the intrinsic relationship between "modification-structure change-adsorption mechanism." The specific model expression is:

$$\ln q_e = \ln q_m - \beta \varepsilon^2 \tag{6}$$

where, $\varepsilon = RT \ln(1+1/C_e)$ is the Polanyi potential, and β is the activity coefficient. The average adsorption energy $E=1/(2\beta)^{1/2}$ can be used to determine the adsorption type: E < 8kJ/mol indicates physical adsorption, and 8kJ/mol < E < 16kJ/mol indicates chemical adsorption. This model is especially useful for distinguishing the nature of adsorption forces of modified zeolites on nitrogen and phosphorus.

The model selection is based on R^2 , χ^2 , and residual analysis, and is judged in conjunction with the physical and chemical significance. This study particularly focuses on how the model fitting results reflect the modification effects on the surface properties of zeolite and how these changes influence the adsorption behavior of nitrogen and phosphorus.

3. RESULTS AND DISCUSSION

To clarify the adsorption rate characteristics and "rate-energy" coupling mechanism of different modified zeolites for nitrogen and phosphorus, adsorption kinetics experiments were conducted, and thermodynamic parameters were correlated. As shown in Table 1, the coefficient of determination for the pseudo-second-order kinetic model of all modified zeolites (0.968–0.995) was significantly higher than that for the pseudo-first-order model, indicating that the adsorption process is primarily chemical adsorption. This result aligns with the conclusion from the D-R model, which suggested "chemical adsorption of PO₄3⁻-P on Fe-based modified zeolites." The pseudo-second-order rate constant of Fe-CTAB-Z (0.0062 g/(mg·min)) was significantly higher than that of other samples, while its ΔH^0 (28.6 kJ/mol) and ΔS^0

(85.2 J/(mol·K)) were the highest, reflecting the "high energy driving high adsorption rate" coupling relationship. The introduction of Fe³+ coordination sites and positively charged surfaces in the composite modification accelerated the adsorption process. Furthermore, the rate control step for Fe-Z involved pore diffusion, matching the structural feature of "increased pore volume" observed in its BET characterization, whereas CTAB-Z predominantly involved surface adsorption, corresponding to its "micropore blockage" in the pore structure. These results confirm that the modification strategy adjusts the adsorption rate by regulating the adsorbent's "surface active sites-pore structure-thermodynamic energy," with the synergistic effect of composite modification being the core mechanism to simultaneously enhance adsorption rate and thermodynamic driving force.

Table 1. Adsorption kinetic parameters of different modified clinoptilolite on nitrogen and phosphorus

Parameter		Raw-Z	Fe-Z	CTAB-Z	Fe-CTAB-Z
Pseudo-First- Order Kinetic Model	Rate Constant (min ⁻¹)	0.012 ± 0.001	0.021 ± 0.002	0.009 ± 0.001	0.028 ± 0.003
	Fitted Equilibrium Adsorption Capacity (mg/g)	7.8 ± 0.3	11.5±0.4	5.9±0.2	17.2±0.5
	Coefficient of Determination	0.896	0.921	0.883	0.935
Pseudo-Second- Order Kinetic Model	Rate Constant (g/(mg·min))	0.0021 ± 0.0002	0.0045 ± 0.0003	0.0018 ± 0.0002	0.0062 ± 0.0004
	Fitted Equilibrium Adsorption Capacity (mg/g)	8.5±0.2	20.3±0.5	6.2±0.2	18.1±0.4
	Coefficient of Determination	0.972	0.993	0.968	0.995
Ra	te Control Step	Pore Diffusion Dominates	Surface Adsorption + Pore Diffusion	Surface Adsorption Dominates	Surface Adsorption (Chemical Coordination) Dominates
Corresponding	Enthalpy Change (kJ/mol)	8.3±0.5	25.3 ± 0.8	12.6 ± 0.6	28.6 ± 1.0
Thermodynamic Parameters	Entropy Change (J/(mol·K))	42.1±2.0	72.5±3.0	45.8±2.0	85.2±3.5

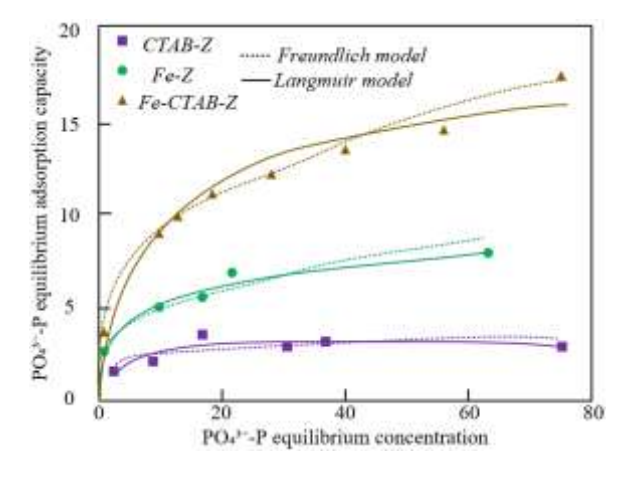


Figure 3. Adsorption isotherms of different modified clinoptilolite for PO₄³⁻-P (298 K)

To clarify the regulation effects of different modification strategies on the adsorption performance of clinoptilolite for PO₄³-P and to reveal the isothermal characteristics of the adsorption behavior, adsorption isotherms for PO₄³-P on modified clinoptilolite were measured at 298 K and fitted to models. As shown in Figure 3, the equilibrium adsorption capacity of Fe-CTAB-Z for PO₄³-P was significantly higher than that of the other samples. When the equilibrium concentration of PO₄³-P reached 80 mg/L, its equilibrium adsorption capacity approached 16 mg/g, followed by Fe-Z. CTAB-Z had the lowest adsorption capacity, approximately 3

mg/g. This result highly matches the structural characteristics of Fe3+ coordination sites and the positively charged surface introduced by the composite modification. Moreover, the Langmuir model fitting curve of all samples showed a significantly better fit to experimental data compared to the Freundlich model, indicating that PO₄³⁻-P was adsorbed predominantly as a monolayer on the modified clinoptilolite surface. These results not only validate the hypothesis that "Fe3+ coordination is the key driving force for enhancing PO₄³⁻-P adsorption, and CTAB's positive charge modification generates a synergistic adsorption effect with Fe³⁺," but also provide experimental support for the calculation of subsequent adsorption thermodynamic parameters and the interpretation of the modification mechanism. Additionally, they confirm that the composite modification strategy can effectively overcome the limitations of single organic/inorganic modifications, achieving efficient capture of PO₄³⁻-P.

To investigate the effect of temperature on the adsorption behavior of different modified clinoptilolite for PO₄³⁻-P and provide baseline isothermal data for the calculation of thermodynamic parameters, multi-temperature adsorption isotherms for PO₄³⁻-P on the raw and modified clinoptilolite were measured at 298 K, 308 K, and 318 K. As shown in Figure 4, the equilibrium adsorption capacity of PO₄³⁻-P on all samples significantly increased with temperature, confirming the endothermic nature of the adsorption process. The adsorption capacity ranking of the modified samples remained consistent at all temperatures: Fe-CTAB-Z > Fe-Z > CTAB-Z > Raw-Z. Notably, Fe-CTAB-Z exhibited the highest

equilibrium adsorption capacity at 318 K, approaching 15 mg/g, much higher than that of the raw clinoptilolite (Raw-Z), directly reflecting the synergistic enhancement effect of Fe³⁺ coordination sites and the positively charged surface of CTAB. Furthermore, the adsorption capacity of Fe-CTAB-Z increased much faster than that of other samples as the equilibrium concentration of PO₄³⁻-P increased, and it approached a high adsorption capacity even at lower equilibrium concentrations, reflecting its stronger adsorption affinity for PO₄³⁻-P. These results not only support the hypothesis that "composite modification can effectively overcome the performance

limitations of single modifications and enhance the adsorption capacity and affinity of clinoptilolite for PO_4^{3-} -P," but also provide isothermal behavior data for the subsequent calculation of ΔH^0 , ΔS^0 , and other thermodynamic parameters. Moreover, they reveal the coupling effect of temperature and modification strategy on the adsorption driving force. The introduction of Fe-based active sites strengthens the positive effect of temperature on adsorption, while CTAB's charge modification further amplifies this temperature-induced enhancement effect.

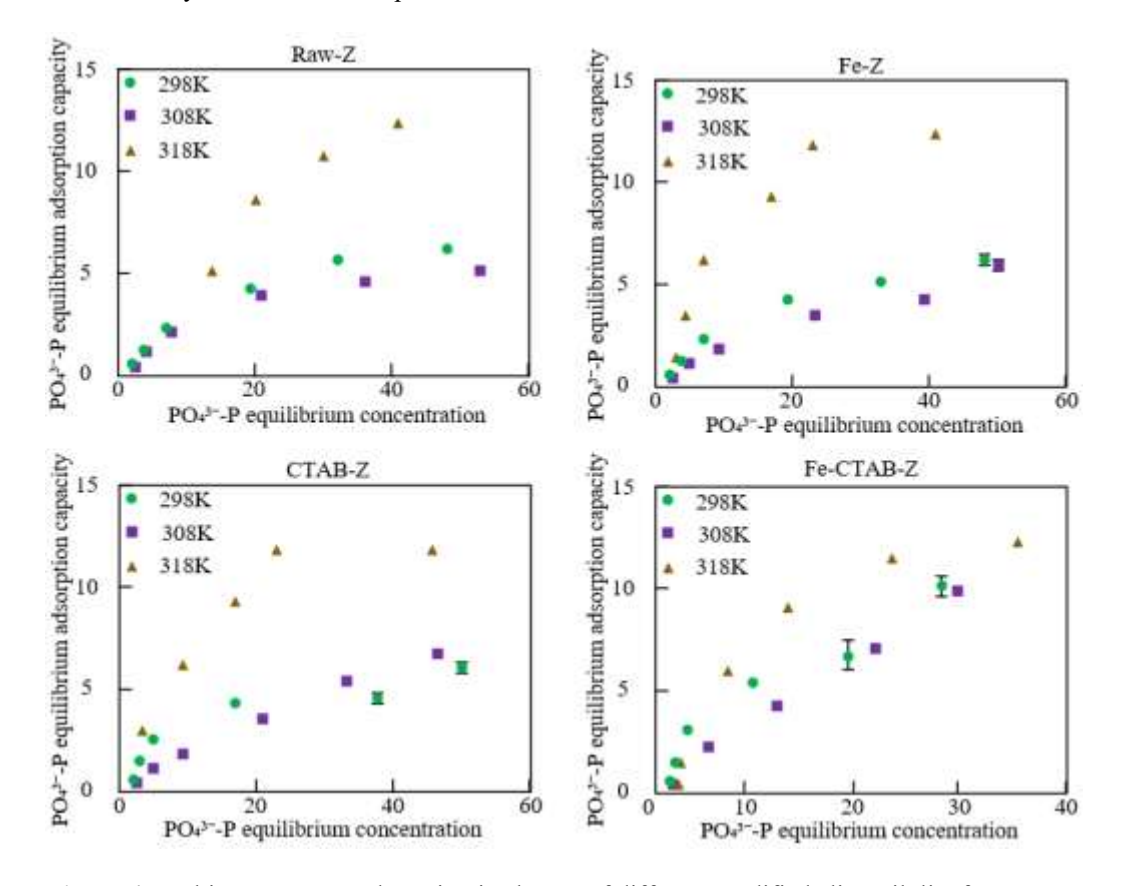


Figure 4. Multi-temperature adsorption isotherms of different modified clinoptilolite for PO₄3--P

Table 2. Effect of pH on the nitrogen and phosphorus adsorption performance of different modified clinoptilolite

Modified Zeolite	pН	NH ₄ ⁺ -N Adsorption	PO ₄ ³⁻ -P Adsorption	Zeta Potential	ΔG^0 (PO ₄ ³⁻ -P,
Type	Group	(mg/g)	(mg/g)	(mV)	kJ/mol)
	pH=3	6.1	1.2	-8.2	-2.1
	pH=5	7.8	1.6	-10.3	-3.5
Raw-Z	pH=7	8.6	1.8	-12.5	-4.2
	pH=9	7.2	1.5	-14.1	-3.3
	pH=11	5.8	1.1	-15.7	-2.0
	pH=3	18.2	9.5	+12.1	-5.6
	pH=5	19.8	11.2	+10.3	-6.3
Fe-Z	pH=7	20.5	12.3	+8.2	-6.8
	pH=9	17.6	10.1	+5.7	-5.2
	pH=11	15.3	8.2	+3.1	-4.0
	pH=3	5.2	4.1	+8.5	-3.8
	pH=5	5.8	4.8	+7.2	-4.5
CTAB-Z	pH=7	6.3	5.2	+5.6	-4.9
	pH=9	5.5	4.6	+3.9	-4.2
	pH=11	4.7	3.9	+2.2	-3.5
	pH=3	16.5	13.2	+14.8	-7.5
	pH=5	17.8	14.5	+13.1	-8.2
Fe-CTAB-Z	pH=7	18.2	15.8	+11.4	-8.8
	pH=9	16.1	13.9	+9.2	-7.3
	pH=11	14.5	12.1	+6.7	-6.1

To clarify the regulation pattern of pH on adsorption performance and the coupling relationship between surface charge, adsorbate form, and thermodynamic spontaneity, this study systematically measured key adsorption thermodynamic parameters at different pH levels. As shown in Table 2, the NH₄⁺-N/PO₄³⁻-P adsorption capacity and ΔG^0 of all modified zeolites reached their peak values at pH=7. For example. Fe-CTAB-Z had its maximum NH₄+-N adsorption of 18.2 mg/g, PO₄³⁻-P adsorption of 15.8 mg/g, and ΔG^0 of -8.8 kJ/mol at pH = 7, which also corresponded to the optimal Zeta potential at neutral pH. This matching originates from the fact that at pH = 7, PO_4^{3-} -P exists primarily as HPO_4^{2-} , and its negative charge density has the strongest electrostatic interaction with the positive surface of Fe-CTAB-Z. At the same time, the coordination bond between Fe³⁺ and HPO₄²⁻ has the highest bond energy, which together enhances the thermodynamic spontaneity of the adsorption process. When the pH deviates from 7, the adsorption behavior shows noticeable changes: at pH=3, PO₄3--P primarily exists as H₂PO₄-, and even though the Zeta potential of Fe-CTAB-Z is higher, its PO₄³⁻-P adsorption of 13.2 mg/g and ΔG^0 of -7.5 kJ/mol are still significantly lower than at pH=7. At pH=11, PO₄³⁻-P exists as PO₄³⁻, but the Zeta potential of the modified zeolite decreases substantially, weakening electrostatic matching, leading to a simultaneous decrease in adsorption capacity and spontaneity. These results further reveal that pH indirectly affects the thermodynamic driving strength of the adsorption process by regulating the "surface charge-adsorbate charge matching. The Fe-CTAB modification strategy enhances the compatibility of surface positive charge density and Fe3+ coordination sites under neutral pH conditions, maximizing the adsorption efficiency driven by thermodynamics.

To quantitatively analyze the thermodynamic driving mechanisms of different modification strategies for NH₄⁺-N and PO₄3--P adsorption on clinoptilolite, the Van't Hoff equation was used to fit the relationship between temperature and adsorption affinity, deriving ΔH^0 and ΔS^0 . As shown in Figures 5 and 6, the lnK_L of all modified zeolites significantly decreases with 1/T, showing a linear trend that conforms to the thermodynamic linear characteristics of the Van't Hoff equation, confirming that temperature regulation of the adsorption constant follows Langmuir the thermodynamic law. For the NH₄+-N system, the slope absolute value of Fe-CTAB-Z's fitting line is significantly smaller than that of Raw-Z, corresponding to a lower ΔH^0 of 12.6 kJ/mol compared to Raw-Z's 18.2 kJ/mol, indicating that the Fe-CTAB composite modification weakens the temperature dependence of NH_4^+ -N adsorption. In the PO_4^{3-} -P system, the absolute value of Fe-CTAB-Z's slope is the largest, corresponding to a ΔH^0 of 28.6 kJ/mol, much higher than Raw-Z's 8.3 kJ/mol, indicating that composite modification enhances the endothermic nature of PO₄³⁻-P adsorption. Additionally, the intercept of Fe-CTAB-Z's fitting line (which is the highest in both systems) indicates that the disorder of the system during adsorption increases the most, which is related to the "Fe3+ coordination sites + CTAB's positive charge surface" synergistically promoting the interfacial exchange of nitrogen and phosphorus ions with water molecules. These results quantitatively support the core conclusion that "modification strategies selectively regulate the thermodynamic behavior of nitrogen and phosphorus adsorption." Composite modification enhances the chemical driving force for PO₄3--P adsorption while reducing the temperature sensitivity of NH₄⁺-N adsorption. They also provide thermodynamic quantification for the interpretation of the adsorption mechanism: the high ΔH^0 of PO₄³-P on FeCTAB-Z corresponds to the chemical coordination interaction between Fe³⁺ and phosphate groups, while the low ΔH^0 of NH₄⁺-N reflects ion-exchange-based physical-chemical coupled adsorption.

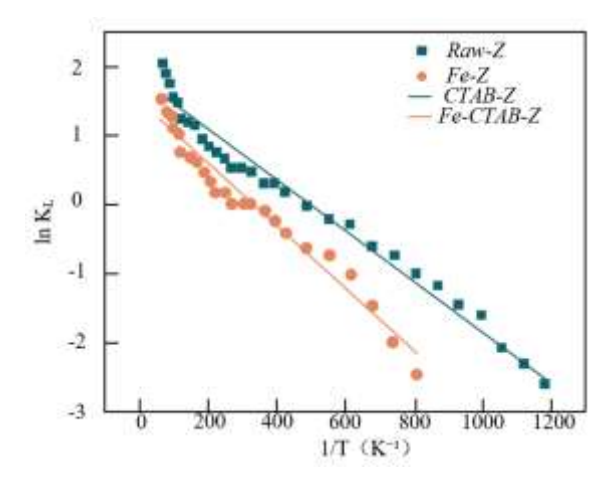


Figure 5. Van't Hoff fitting plot of PO₄³⁻-P adsorption on different modified clinoptilolite

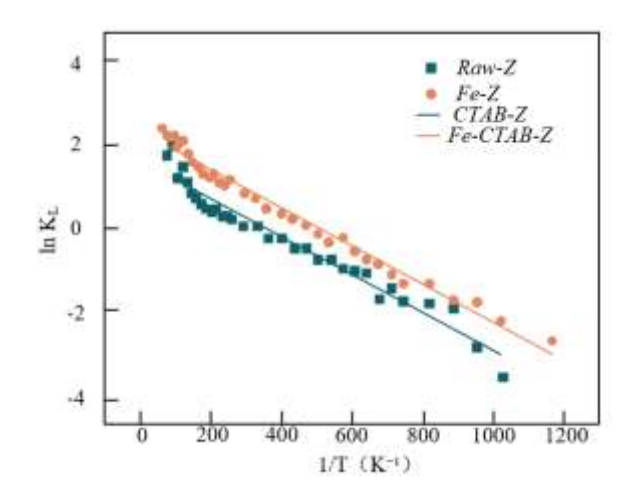


Figure 6. Van't Hoff fitting plot of NH₄+-N adsorption on different modified clinoptilolite

4. CONCLUSION

This study systematically explored the regulation effects of inorganic modification with FeCl₃, organic modification with CTAB, and composite modification (Fe-CTAB) on the nitrogen and phosphorus adsorption performance of clinoptilolite. Through structural characterization using XRD, SEM, BET, FTIR, Zeta potential, XPS, and the coupling of adsorption kinetics, multi-temperature isotherms, and pH influence experiments, thermodynamic parameters were used to clarify the adsorption mechanism. The study shows that the modification strategy optimizes adsorption performance by directing the regulation of surface active sites, pore structure, and charge properties of clinoptilolite: the introduction of Fe³⁺ constructs a porous structure through lattice insertion and oxide loading, providing chemical coordination sites, while CTAB enhances the surface positive charge density through

quaternary ammonium groups. The composite modification forms a synergistic effect of "porous-positive charge-multiple active sites," significantly improving the maximum adsorption capacity of Fe-CTAB-Z for PO₄3--P compared to single modifications and raw zeolite. For NH4+-N, due to slight micropore blockage by CTAB, Fe-Z is slightly better than Fe-CTAB-Z. Kinetic fitting confirmed that the adsorption is dominated by chemical adsorption, and thermodynamic parameters showed that all adsorption processes are spontaneous and endothermic. Fe-CTAB-Z had the highest ΔH^0 (28.6 kJ/mol) and ΔS^0 (85.2 J/(mol·K)), confirming the synergistic effect of chemical coordination and electrostatic adsorption. pH influence experiments further clarified that the adsorption performance of all samples was optimal at pH=7. Fe-CTAB-Z showed a wider pH application range due to the synergistic effect of charge compatibility and coordination. This research not only proposes an efficient strategy of "inorganic-organic composite modification to enhance nitrogen and phosphorus adsorption on clinoptilolite," but also, through "structural characterization-performance testingthermodynamic/kinetic coupling" systematic analysis, reveals structure-performance-thermodynamic relationship, providing theoretical guidance and technical support for the directed modification of low-cost mineral adsorbents and the control of nitrogen and phosphorus pollution in water bodies.

Although this study clarified the nitrogen and phosphorus adsorption mechanisms and performance advantages of modified clinoptilolite, certain limitations remain: first, the evaluation of adsorption performance is mainly based on simulated wastewater systems, and the interference mechanisms of high-concentration coexisting ions in real water bodies on adsorption selectivity have not been fully clarified; second, although the synergistic effect of composite modification has been confirmed, the global optimization of modification parameters and cost control has not been deeply explored, and the lack of data on the adsorption agent's cyclic regeneration performance limits its quantitative evaluation of engineering applications; third, the explanation of the adsorption mechanism relies on static characterization, lacking in situ dynamic characterization to track the real-time evolution of ion diffusion and bonding during the adsorption process, and the accuracy of the microscopic mechanism needs further validation. Based on this, future research could focus on three aspects: first, expanding to actual complex water bodies such as aquaculture wastewater and municipal tailwater to explore the interference mechanisms of coexisting ions and optimize the adsorption process; second, using global optimization tools such as response surface methodology to parameters low-cost modification determine systematically evaluate the cyclic regeneration performance and long-term stability of the adsorbent; third, combining in situ characterization technologies with molecular simulations to deepen the "ion-active site-pore interaction" mechanism from a dynamic perspective, providing more direct theoretical support for the precise design and performance enhancement of adsorbents.

REFERENCES

[1] Nikolaidis, N.P., Phillips, G., Poikane, S., Várbíró, G., Bouraoui, F., Malagó, A., Lilli, M.A. (2022). River and lake nutrient targets that support ecological status:

- European scale gap analysis and strategies for the implementation of the Water Framework Directive. Science of the Total Environment, 813: 151898. https://doi.org/10.1016/j.scitotenv.2021.151898
- [2] Llorens, B., Pomar, C., Goyette, B., Rajagopal, R., Andretta, I., Latorre, M.A., Remus, A. (2024). Precision feeding as a tool to reduce the environmental footprint of pig production systems: A life-cycle assessment. Journal of Animal Science, 102: skae225. https://doi.org/10.1093/jas/skae225
- [3] Wałęga, A., Chmielowski, K., Młyński, D. (2019). Nitrogen and phosphorus removal from sewage in biofilter–activated sludge combined systems. Polish Journal of Environmental Studies, 28(3): 1939-1947. https://doi.org/10.15244/pjoes/89898
- [4] Chi, R., Wei, Z., Gong, L., Zhang, G., Wen, D., Li, W. (2024). The study of nitrogen and phosphorus removal efficiency in urbanized river systems using artificial wetland systems with different substrates. Water, 16(22): 3309. https://doi.org/10.3390/w16223309
- [5] Sun, H., Shen, B., Liu, J. (2008). N-Paraffins adsorption with 5A zeolites: The effect of binder on adsorption equilibria. Separation and purification technology, 64(1): 135-139. https://doi.org/10.1016/j.seppur.2008.08.013
- [6] Krishna, L.S., Soontarapa, K., Asmel, N.K., Kabir, M.A., Yuzir, A., Zuhairi, W.W., Sarala, Y. (2019). Adsorption of acid blue 25 from aqueous solution using zeolite and surfactant modified zeolite. Desalination and Water Treatment, 150: 348-360. https://doi.org/10.5004/dwt.2019.23726
- [7] Vosmerikov, A.A., Vosmerikova, L.N., Vosmerikov, A.V. (2024). Studying the influence of alkaline treatment and modification of zeolite on its physical-chemical and catalytic properties in the process of propane conversion to olefin hydrocarbons. Izvestiya Vysshikh Uchebnykh Zavedeniy Khimiya Khimicheskaya Tekhnologiya, 67(8): 50-58. https://doi.org/10.6060/ivkkt.20246708.11t
- [8] Goworek, J., Stefaniak, W., Zaleski, R. (2019). Study of swollen crosslinked polymers by low-temperature adsorption of nitrogen using blocking siloxane agent. Polymer Testing, 79: 105990. https://doi.org/10.1016/j.polymertesting.2019.105990
- [9] Saka, C., Teğin, İ., Kahvecioğlu, K., Yavuz, Ö. (2024). Nitrogen-and oxygen-doped carbon particles produced from almond shells by hydrothermal method for efficient Pb (II) and Cd (II) adsorption. Biomass Conversion and Biorefinery, 14(15): 17467-17480. https://doi.org/10.1007/s13399-023-03920-8
- [10] Wu, D., Sun, Y., Wang, L., Zhang, Z., Gui, J., Ding, A. (2020). Modification of NaY zeolite by lanthanum and hexadecyl trimethyl ammonium bromide and its removal performance for nitrate. Water Environment Research, 92(7): 987-996. https://doi.org/10.1002/wer.1285
- [11] Xiao, F. S., Zheng, S., Sun, J., Yu, R., Qiu, S., Xu, R. (1998). Dispersion of inorganic salts into zeolites and their pore modification. Journal of catalysis, 176(2): 474-487. https://doi.org/10.1006/jcat.1998.2054
- [12] Rakhym, A.B., Seilkhanova, G.A., Mastai, Y. (2021). Physicochemical evaluation of the effect of natural zeolite modification with didodecyldimethylammonium bromide on the adsorption of Bisphenol-A and Propranolol Hydrochloride. Microporous and Mesoporous Materials, 318: 111020.

- https://doi.org/10.1016/j.micromeso.2021.111020
- [13] Kalaiselvi, D., Renuka, R. (2000). Zeolite modification of organic cathodes: Clean technology for improved cycle life of the zinc-chloranil organic secondary battery. Journal of Chemical Technology & Biotechnology, 75(4): 285-293. https://doi.org/10.1002/(SICI)1097-4660(200004)75:4%3C285::AID-JCTB207%3E3.0.CO:2-C
- [14] Toommee, S., Pratumpong, P. (2018). PEG-template for surface modification of zeolite: A convenient material to the design of polypropylene based composite for packaging films. Results in Physics, 9: 71-77. https://doi.org/10.1016/j.rinp.2018.02.006
- [15] Quiroga, E., Ramirez-Pastor, A.J. (2013). Statistical thermodynamics of molecules with multiple adsorption states: Application to protein adsorption. Chemical Physics Letters, 556: 330-335. https://doi.org/10.1016/j.cplett.2012.11.019
- [16] Shkilev, V.P., Lobanov, V.V. (2017). Thermodynamics of adsorption on deformable adsorbents. Russian Journal of Physical Chemistry A, 91(4): 758-765.

- https://doi.org/10.1134/S0036024417040276
- [17] Han, B., Chen, W., Wang, C.X., Li, L., Yan, H., Li, W.X. (2010). Adsorption thermodynamics of isoliquiritin on multi-walled carbon nanotubes. Carbon, 48(7): 2126-2126. https://doi.org/10.1016/j.carbon.2010.01.048
- [18] Sayan, E., Ata, O.N., Edecan, M.E. (2014). Investigation of adsorption thermodynamics on removal of reactive blue 19 onto activated carbon under ultrasonic irradiation. Journal of the Chemical Society of Pakistan, 36(2): 232-238.
- [19] Riccardi, C.C., Borrajo, J. (1993). Epoxy/amine systems with monodisperse modifiers: thermodynamic analysis of the phase separation process taking the polymer polydispersity into account. Polymer International, 32(3): 241-246. https://doi.org/10.1002/pi.4990320305
- [20] Rico, M., López, J., Montero, B., Bouza, R., Díez, F.J. (2014). Influence of the molecular weight of a modifier on the phase separation in an epoxy thermoset modified with a thermoplastic. European Polymer Journal, 58: 125-134.
 - https://doi.org/10.1016/j.eurpolymj.2014.06.017